

An Accurate ECG Based Transportation Safety Drowsiness Detection Scheme

Kwok Tai Chui, *Student Member, IEEE*, Kim Fung Tsang, *Senior Member, IEEE*, Hao Ran Chi, *Student Member, IEEE*, Bingo Wing Kuen Ling, *Senior Member, IEEE*, and Chung Kit Wu

Abstract—Many traffic injuries and deaths are caused by the drowsiness of drivers during driving. Existing drowsiness detection schemes are not accurate due to various reasons. To resolve this problem, an accurate driver drowsiness classifier (DDC) has been developed using an electrocardiogram genetic algorithm based support vector machine (ECG GA-SVM). In existing studies, a cross correlation kernel and a convolution kernel have both been applied for performing the classification. The DDC is designed by a Mercer kernel K_{DDC} formed by commuting the cross correlation kernel ($K_{xcorr,ij}$) and the convolution kernel ($K_{conv,ij}$). $K_{xcorr,ij}$ captures the symmetric information among ECG signals from different classes, while $K_{conv,ij}$ captures the anti-symmetric information among ECG signals from the same class. The final K_{DDC} (a pre-computed kernel) is obtained by a genetic mutation using a multi-objective genetic algorithm. This renders an optimal K_{DDC} that confidently serves as the full descriptor of the drowsiness. The performance of K_{DDC} is compared to the most prevailing kernels. The obtained DDC yields an overall accuracy of 97.01%, sensitivity of 97.16%, and specificity of 96.86%. The analysis reveals that the accuracy of K_{DDC} is better than those of both $K_{xcorr,ij}$ and $K_{conv,ij}$ by more than 11%, and typical kernels including linear, quadratic, third order polynomial and Gaussian radial basis function by 17% to 63%, respectively. Comparing to related works using the image based method and the biometric signal based method, K_{DDC} improves the accuracy by 48.4% to 87.2%, respectively. Testing results showed that K_{DDC} has less than 1% deviation from simulated results. Also, the average delay of DDC was bounded by 0.55ms. This renders the real time implementation. Thus, the developed ECG GA-SVM provides an accurate and instantaneous warning to the drivers before they fall into sleep. As a result this ensures the public transport safety.

Index Terms—Drowsiness detection, electrocardiogram, genetic algorithm, optimization, pre-computed kernel, support vector machine, transportation safety.

Manuscript received July 1, 2015; revised February 19, 2016; Accepted March 24, 2016.

Copyright (c) 2011 IEEE. Personal use of this material is permitted. However, permission to use this material for any other purposes must be obtained from the IEEE by sending a request to pubs-permissions@ieee.org.

K. T. Chui, K. F. Tsang, H. R. Chi and C. K. Wu are with the Department of Electronic Engineering, City University of Hong Kong, Kowloon, Hong Kong SAR (e-mail: ktchui3-c@my.cityu.edu.hk, ee330015@cityu.edu.hk, haoranchi2-c@my.cityu.edu.hk, chungkwu4-c@my.cityu.edu.hk).

B. W. K. Ling is with Guangdong University of Technology, Guangzhou, Guangdong, China (e-mail: yongquanling@gdut.edu.cn).

I. INTRODUCTION

REPORTS from the World Health Organization revealed that nearly 1.3 million people were killed and 50 million people were injured in road traffic collisions each year. These accidents and injuries imposed a very heavy burden to healthcare industries and hospitals [1]. It is estimated that 1% to 3% of the respective GDP of the world (more than \$500 billion) will be spent on traffic crashes [2]. It is expected that accidents will double the car insurance premium in five years. Since the number of motor vehicles is ever increasing, the leading cause of death will soar from the 9th to the 5th position by 2030 if no precautionary measures are devised.

Poor fatigue conditions of drivers such as sleep, drink, drug, sudden illness or mental defect is the major causes of traffic accidents. In the U.S., drowsy drivers cause about 56,000 car crashes with thousands of mortalities and 40,000 of injuries every year [3]. Statistics also revealed that 60% of adult drivers felt sleepy while driving and 37% of them fell asleep [4].

Driver's drowsiness may potentially cause sleepiness which presents an unfavorable condition. Engineers and scientists have been devoting a lot of efforts on developing techniques for the precise detection of drowsiness. In this investigation, an attention is drawn to the accurate detection of drowsy drivers. Once the drowsiness is detected, in general request commands will be sent to the central server as well as simultaneously alarm warnings will be sent to the driver and for managing the alert and remedial purposes.

Few drowsiness detection approaches were proposed for the detection of drowsy drivers. There are three types of drowsiness detections. The first two methods are non-intrusive, namely an image based method [5]-[8] and a vehicle based method [9]-[11]. The third detection method is a biometric signal based method which is intrusive [12]-[16].

Related works for the driver's cognitive distraction detection [17] is not the main focus of this paper. This is because this application is differed from this one. Another work has focused on the driver drowsiness detection using 5 drowsiness level ratings [18]. Since the decision is made by the raters' intuition, it may not be reliable from the practical usage viewpoint.

On the other hand, there may be confusion between the driver fatigue detection [19], [20] and the driver drowsiness detection. The driver fatigue detection detects the level of fatigue in which they may not be drowsy or even fall asleep. When it comes to

fatigue, a large portion of people enters the fatigue status. However, they are able to drive safely because they are conscious. Hence, it is worth to focus on the detection of the drowsy status since the drivers drive unconsciously. To address this problem, the heart rate variability (HRV) is used as a feature for the detection [19], [20]. However, the HRV is obtained from the RR-intervals of ECG signal, which is a single point, R in the ECG signal. On the other hand, the ECG signal is characterized by the P wave, QRS wave and T wave. In this paper, each ECG signal contains 100 samples. It contains much more information than the heart rate.

A low measurement resolution may result to a fake indicator of “driving”. Besides, the measurement stability is a very important factor since each measurement point must truly reflect and indicate the intrinsic human property. In an investigation on the data reliability of the ECG, the eye blinking signal and the EEG under different driving conditions, the score for the ECG signal measurement is ~97.5% [16]. On the other hand, the score for the eye blinking signal is only 58.75% and that of the EEG signal is 85%. Thus, it can be concluded from this investigation that the ECG signal provides the highest reliability. Both the ECG signals itself and its reliability confirm that the ECG signal is the most reliable and accurate indicator for the *sleepiness* [16]. Thus, this paper employs the ECG signal for the detection.

There are also some works [21] on the acquisitions of the ECG signals via non-traditional sensors such as the textile capacitive ECG electrodes and the steering wheels with the integrated physiological sensors. This reference is provided to readers who are interested in the data acquisitions.

An ECG based classifier for the driver drowsiness detection was proposed [22]. The cross correlation coefficients were employed as a feature vector. The radial basis kernel function was used for performing the classification. It yields an overall accuracy, sensitivity and specificity of 76.93%, 77.36% and 76.5%, respectively. Hitherto, the precise ECG detection method for the drowsiness detection is not available. Inspired by the quality of service from a network design, a typical accuracy error and the reliability deviation error have to be bounded within 5%.

Traditionally, there are several stages of sleep, namely the sleep stage 1, the sleep stage 2, the sleep stage 3, the sleep stage 4 and the rapid eye movement (REM) [23]. To facilitate an efficient detection of the drowsiness, only the sleep stage 1 and the sleep stage 2 will be considered in this research. This investigation proposes three classifiers, namely the classifier 0, the classifier 1 and the classifier 2, for the drowsiness detection based on ECG signals. The pre-computed kernel K_{DDC} distinguishes among these three driving statuses, namely the awake state, the sleep stage 1 and the sleep stage 2. These three classifiers are defined as Classifier 0 which is used for the classification between the driving awake stage and the sleep stage 1; Classifier 1 which is used for the classification between the driving awake stage and the sleep stage 2; and Classifier 2 which is used for the classification between the sleep stage 1 and

the sleep stage 2. The sleep stage 1 and the sleep stage 2 are referred as the *light sleep*.

(i) Sleep stage 1 [23]: The driver’s condition is considered as a transition between the *awake* stage and the *sleep* Stage 1. This is the early stage to enter the drowsiness from the *awake* stage. Also, the drowsy period may vary from person to person. It ranges from few seconds to few minutes. The classifier for distinguishing between the “awake” stage and the “sleep stage 1”, is performed by the classifier 0, as shown in Fig. 1.

(ii) Sleep stage 2 [23]: In this stage, the body temperature and the heart rate will decrease. The drowsy sleep may be last from few minutes to 20 minutes. The classifier for distinguishing between the “awake” stage and the “sleep stage 2” is performed by the classifier 1 as shown in Fig. 1.

(iii) Each of the classifier (classifier 0, classifier 1 and classifier 2) has its decision boundary. These decision boundaries form the decision region of DDC. The proposed DDC gives a decision according to the driver states (awake state, the sleep stage 1 and the sleep stage 2), adaptively.

Thus, an accurate detection based on the classifier 0 and classifier 1 may provide an early warning to the driver for avoiding potential accidents.

Fig. 1 shows the transitions among the driving awake state, the sleep stage 1 and the sleep stage 2 by the classifier 0, classifier 1 and classifier 2 of K_{DDC} . There are three possible states for the driver. They are the awake state, the sleep stage 1 and the sleep stage 2. The state diagram for the activation of the classifiers is shown in Fig. 2. In the awake state, the classifier 0 and the classifier 1 are activated. In the sleep stage 1, the classifier 2 is activated. In the sleep stage 2, all the classifiers are turned off. A warning alarm will be made to awake the driver either in the sleep stage 1 or the sleep stage 2. Hence, there are return paths from the sleep stage 1 to the awake state and from the sleep stage 2 to the awake state as shown in the state diagram. It is important to point out that both C0 and C1 are activated in the awake state since sleep stages may go from two different cases. The first case is from the awake state to the sleep stage 1 and the second case is from the awake state to the sleep stage 2. For the second case, it occurs directly from the awake state if the driver has the sleep deprivation. In this case, the sleep stage 1 is skipped and the driver will go to the REM state quickly.

It should be noted that the sleep stage 3, the sleep stage 4 and the REM stage are not considered in this paper since these stages are categorized as the deep sleep stages. This implies that the driver has slept for more than 10 minutes and accident may have already occurred.

An accurate driver drowsiness classifier (DDC) has been developed by using an electrocardiogram genetic algorithm based support vector machine (ECG GA-SVM). The SVM is a very powerful tool for performing the classification and has found many applications [24]. To perform an accurate and efficient classification among the awake stage, the sleep stage 1 and the sleep stage 2, an optimal design of the K_{DDC} is required. For achieving an accurate drowsiness detection, the cross correlated ($K_{corr,ij}$) and the convoluted ($K_{conv,ij}$) ECG signals

will be computed for capturing both the symmetric and asymmetric information for the classification of the awake state, the sleep stage 1 and the sleep stage 2. This information is a robust indicator for the drowsiness detection. The most accurate, efficient and highly correlated kernel will be defined by finding a solution of a multi-objective optimization problem using a genetic algorithm. Classifier 0, classifier 1 and classifier 2 have been analyzed and evaluated.

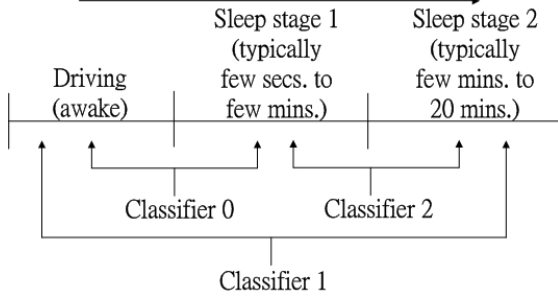


Fig. 1. Relationships among classifier 0, classifier 1 and classifier 2 of K_{DDC} .

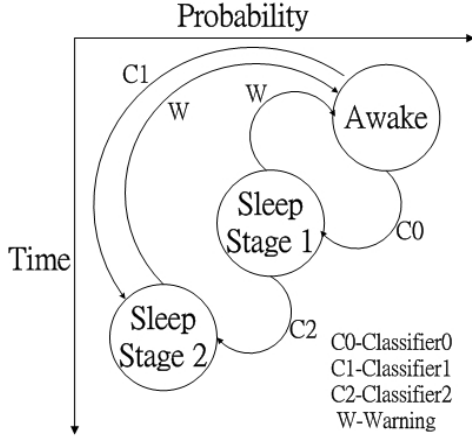


Fig. 2. State diagram for driver drowsiness detection.

By using the ECG GA-SVM, the DDC yields an overall accuracy of 97.01%, sensitivity of 97.16% and specificity of 96.86%. The analysis reveals that the accuracy of K_{DDC} is better than those of $K_{xcorr,ij}$ and $K_{conv,ij}$ kernels by more than 11%. Compared to prevailing kernel functions, the K_{DDC} yields higher overall accuracies by 17% to 63%. Also, the K_{DDC} significantly increases the equivalent accuracies by 48.4% and 87.2% compared to the related works using the image based and the biometric signal based methods, respectively. Comparison to the testing results, the performance obtained by our proposed DDC is within 99% agreement with that of the simulated results. Further analysis on the latency shows that the average delay of Classifier 0, Classifier 1, and Classifier 2 is 0.534ms, 0.549ms and 0.54ms, respectively. The detection can be performed in “real time”. Such performance concludes that the required computation time is negligible. Thus, it is practical for industrial applications.

The organization of this paper is as follows. The overview of the driver drowsiness system is discussed in Section II. Section III describes the methodology of formulating the pre-computed kernel with an optimal correlation analysis. Section IV evaluates the performance of the system and presents the results with the comparisons to related works. Finally, a conclusion is

drawn in Section V.

II. PROCEDURE FOR PAPER SUBMISSION

Fig. 3 shows the flow chart of DDC. The system is activated when the vehicle starts moving. The DDC is responsible for the classification among the awake stage, the sleep stage 1 and the sleep stage 2. It should be pointed out that the DDC does not detect the normal wake-up. The ECG signal of the driver is measured and then signal pre-processing operations are carried out. The pre-processing operations include the dc drift elimination, the digital lowpass filtering (LPF) and the highpass filtering (HPF). Next, the R waves are detected based on the QRS complex detection. Here, the whole ECG sequences are segmented into individual pieces of consecutive R waves. The P wave and the T wave are not used for the ECG beat segmentation. This is because they are sensitive to noise and they result to achieve lower detection accuracies [25]. Afterwards, the convolution and the cross-correlation are applied between two individual signals and their optimal coefficients are computed for constructing the testing kernel. The trained DDC processes the ECG and gives the current status of the driver as the awake stage, the sleep stage 1 or the sleep stage 2. A warning message such as a buzz sound will be generated if the driver is in the sleep stage 1 or in the sleep stage 2. The status of the driver will be updated and the whole process keeps repeating continuously.

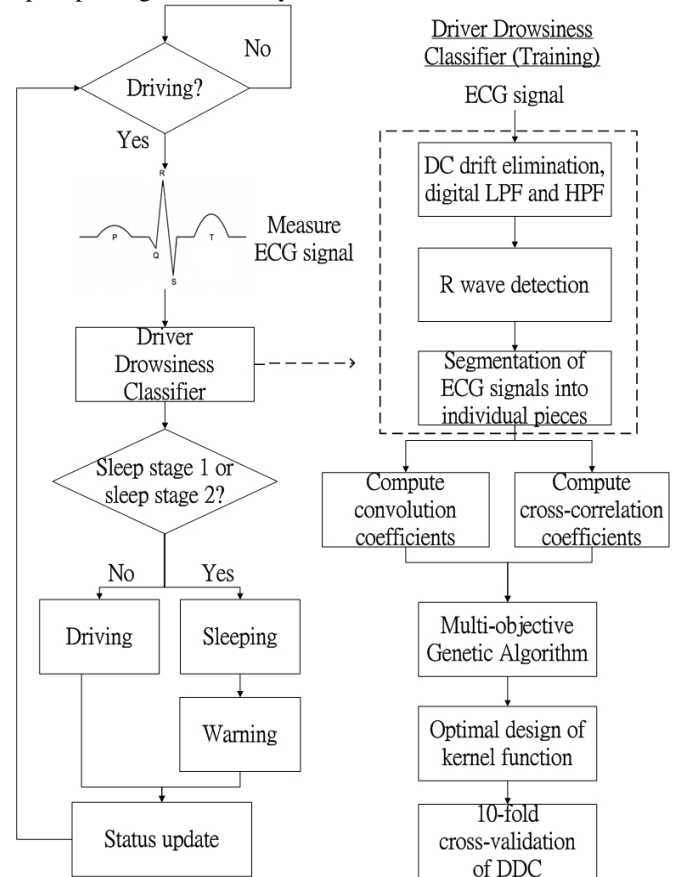


Fig. 3. Flow chart showing the construction of the driver drowsiness system.

The development of the DDC is summarized below. An ECG database is utilized [26] for the training purpose. The ECG database consists of ECG signals from both sleepy and awake drivers. The above signal pre-processing operations are applied. The convolution and the cross-correlation coefficients are then calculated. An optimal set of weighting factors is evaluated using the genetic algorithm. As a result, the pre-computed kernel K_{DDC} is obtained. The reason why the pre-computed kernel is employed instead of using feature extracted based on prevailing typical kernels will be explained in section II C. The kernel is very crucial for the drowsiness identification via the DDC. To obtain a holistic view, the pre-computed kernel will be developed and analyzed. The obtained performance is compared to typical kernels such as the linear, quadratic, polynomial and Gaussian radial basis function (RBF). A benchmark analysis will be discussed.

III. DESIGN OF DRIVER DROWSINESS CLASSIFIER (DDC): PRE-COMPUTED KERNEL WITH OPTIMAL CORRELATION ANALYSIS

In this section, the database of the ECG signals from both the awake and drivers are discussed. Then, the signal preprocessing operations will be presented. Next, the optimal design of K_{DDC} based on the correlation analysis and the genetic algorithm are developed. Finally, the DDC is constructed according to the developed K_{DDC} . Table I summarizes the notations of the variables used in this paper.

A. Database of ECG Signals

All the ECG signals of the awake drivers and the sleepy drivers taken out from the Stress Recognition in Automobile Drivers Database (SRDB) and from the CinC The CAP Sleep Database (CSD) are used [26]. The SRDB includes 18 records. 16 records have durations between 65 and 93 minutes and the remaining two records last for 25 and 29 minutes. These records were captured under the real world city and highway driving conditions. In CSD, 108 records are obtained from sleep centers. These records contain signals from drivers in six sleep stages. They are the awake stage, the sleep stage 1, the sleep stage 2, the sleep stage 3, the sleep stage 4 and the rapid eye movement (REM) stage. The definitions of these stages can be referred to [23].

For the practical reason, only ECG signals at the sleep stage 1 and the sleep stage 2 are considered. In the design of K_{DDC} , the datasets are further divided into three classes. They are the Class 0 corresponding to the awake stage, the Class 1 corresponding to the sleep stage 1 and the Class 2 corresponding to the sleep stage 2. Each class contains 20000 samples with one ECG beat per sample. Therefore, the total number of samples is 60000. Using the same number of samples in each class can avoid the occurrence of the case where the SVM requires a specific class having a huge number of samples for training [27]. It should be pointed out that each ECG beat lasts for 0.6 to 1 second. For the signal sampled at 100Hz, the signal length is with 60 to 100 points. The zero padding approach is employed when the signal length is less than 100. Thus, all the samples in each class have

the length of 100 for each ECG beat.

Table I. Notations of the variables used in this paper.

Variable notation	Description
$H_{low}(z)$	Transfer function of the lowpass filter
$H_{high}(z)$	Transfer function of the highpass filter
$h_d(n)$	Impulse response of the derivative filter
$y(nT)$	Integration via a moving window
NPKE	Running estimate of the noise peak
SPKE	Running estimate of the signal peak
PEAKE	Overall peak
$X_{i,j}(n)$	The j^{th} ECG signal from the class i set
$R_{p,q}^{i,j}(n)$	Cross-correlation coefficients between $X_{i,j}(n)$ and $X_{p,q}(n)$
$C_{p,q}^{i,j}(n)$	Convolution coefficients between $X_{i,j}(n)$ and $X_{p,q}(n)$
$\omega_{xcorr,ij,m}$	Weighting factors of $R_{p,q}^{i,j}(n)$
$\omega_{conv,ij,m}$	Weighting factors of $C_{p,q}^{i,j}(n)$
$K_{conv,ij}$	Convolution based kernel matrix
$K_{xcorr,ij}$	Cross correlation based kernel matrix
K_{DDC}	Kernel matrix of DDC
$X_{conv,i,j}$	Weighted sum of the convolution coefficients between the ECG signal from the class i set and the class j set
$X_{xcorr,i,j}$	Weighted sum of the cross correlation coefficients between the ECG signal from the class i set and the class j set
N_t	Total number of training data
F_1	Objective 1
F_2	Objective 2
$\tilde{M}(\alpha, \omega)$	Maximum margin function
α_i	Lagrange multiplier
OA	Overall accuracy
Se	Sensitivity
Sp	Specificity
TP	True positive
TN	True negative
FP	False positive
FN	False negative

B. Data Preprocessing

Aforementioned, the beat segregation is performance on the ECG signals. Each ECG frame is defined as a signal between two consecutive R waves and it forms an individual sample. The reason for not choosing P wave and T wave is that they are noise sensitive and it results to low beat segregation accuracy [24].

Thus, a popular Tompkins QRS complex detection algorithm with the reliable accuracy larger than 99% is chosen [28], [29]. The methodology is summarized as follows [29]:

The frequency of the QRS complex is ranged between 10 and 30Hz. A cutoff frequency is selected at 11Hz. The ECG signal is then processed by a linear phase low-pass filter with the transfer function $H_{low}(z)=(1-z^{-6})^2/(1-z^{-1})^2$ so that the 60Hz muscle noise and the power line interference are suppressed. The gain and the delay of the lowpass filter are 31.1dB and 5 samples, respectively. The 60Hz muscle noise is attenuated by 35dB.

After that, the signal is processed by a high-pass filter with the transfer function $H_{high}(z)=z^{-16}-H_{low}(z)/32$. The low cutoff frequency of the high-pass filter is 5Hz and the delay of filter is 16 times of its sampling period.

The linear phase derivative filter is then used to determine the slope information of the QRS complex. The detectable frequency can be up to 30Hz. The filter amplifies the QRS complex and attenuates the high frequency components. The impulse response of the filter $h_d(n)$ is $h_d(0)=-1$, $h_d(1)=-2$, $h_d(3)=2$ and $h_d(4)=1$. The gain and delay of the lowpass filter are 14.3dB and 2 samples, respectively.

The signal squaring and the moving integration are applied to the filtered signal. The difference equation for moving the window integration is

$$y(nT)=[x(nT-(N-1)T)+x(nT-(N-2)T)+\dots+x(nT)]/N,$$

where N is to the total number of samples in the width of the moving window. The starting point of the output is at the location of the Q wave and the width of the output is equal to $2QS$ + the width of the window. Two sets of thresholds have been applied to the ECG signal processed by the moving window integration. Define PEAKI as the overall peak, SPKI as the running estimate of the signal peak and NPKI as the running estimate of the noise peak.

(i) Threshold 1=NPKI+(SPKI-NPKI)/4

where

$$NPKI=PEAKI/8+7(NPKI/8)$$

if PEAKI is the signal peak and

$$SPKI=PEAKI/8+7(SPKI/8)$$

if PEAKI is the noise peak;

(ii) Threshold 2=(Threshold 1)/2.

Thus, the locations of Q, R and S waves of the ECG signals can be obtained. The ECG frame is obtained by segmenting the signals between two consecutive R waves.

Another approach based on wavelet transform also achieves accuracy larger than 99% which is for readers' interest [29].

Some selected distributions of (i) the value of the Q wave, (ii) the value of the R wave, (iii) the value of the S wave and (iv) the duration of the QRS complex of the ECG frames are shown in Fig. 4. From Fig. 4a and Fig. 4c, it can be seen that the variations of the ECG frames among these three classes are small. For the distribution of the R waves, it can be seen from Fig. 4b that the changes between these three classes are large. The distributions move toward the left hand side when the class moves from the awake stage to the sleep Stage 1 and the sleep Stage 2. Also, the voltage of the sleep stage 2 is the smallest, while that of the

awake stage is the highest. In other words, the average value of the sleep stage 2 is the smallest and that of the awake stage is the highest. Similar observation can be seen for the QRS complex. In Fig. 4d, the duration of the QRS complex in the sleep stage 2 is the smallest while that of the awake stage is the highest.

It can be concluded that the QRS complex is significantly different among the awake stage, the sleep stage 1 and the sleep stage 2 since the R waves and the QRS complex durations are different among these three classes. Thus, the features extracted from the ECG signal can be used for the drowsiness detection of drivers.

C. Optimal Designs of Pre-computed kernel of DDC

Aforementioned in Section II, the rationale of adopting the pre-computed kernel for performing the feature extraction is explained below. A similarity kernel is a function defined over the pairs of data. General speaking, a proper kernel has to satisfy the positive semi-definite requirement of the Mercer's theorem. Thus, the similarity kernel of the DDC is optimally designed via the cross correlation and the convolution of the ECG signals. The cross correlation kernel measures the symmetric information among the ECG signals from different classes. For the convolution kernel, it measures the anti-symmetric information among the ECG signals from the same classes. By combining these two kernels, K_{DDC} captures both the symmetric and the anti-symmetric information of the ECG signals. Hence, it can achieve a better performance compared to the case where either the cross correlation kernel or the convolution kernel is used.

The optimal design of the pre-computed kernel is formulated as a multi-objective optimization and a genetic algorithm [30] is used for solving the solution of the optimization problem.

It is notated that the length of $X_{i,j}(n)$ is 100. It refers to the j^{th} ECG signal from the class i set for $i=0,1,2$ and for $j=1,\dots,20000$. Thus, the set of ECG signals in Class 0 is $\{X_{0,1}(n),\dots,X_{0,20000}(n)\}$, that in Class 1 is $\{X_{1,1}(n),\dots,X_{1,20000}(n)\}$ and that in Class 2 is $\{X_{2,1}(n),\dots,X_{2,20000}(n)\}$. The similarity between the ECG signals $X_{i,j}$ and $X_{p,q}$ is defined by the cross correlation as follows:

$$R_{p,q}^{i,j}(k) = \begin{cases} \sum_{n=k}^{L-1} X_{i,j}(n) X_{p,q}(n-k), & k \geq 0, \\ \sum_{n=0}^{L-|k|-1} X_{i,j}(n) X_{p,q}(n-k), & k < 0, \end{cases} \quad (1)$$

where $L=100$ is the length of $X_{i,j}(n)$ for i , for j , for $p=0,1,2$ and for $q=1,\dots,20000$. It has been shown that a set of higher cross correlation values of the ECG signals from the same class is obtained since they are similar in nature. Likewise, a set of lower cross correlation values of the ECG signals from different classes is obtained for the vice versa reason.

For the same values of L , i , j , p and q , the convolution between the ECG signal $X_{i,j}(n)$ and $X_{p,q}(n)$ is defined as:

$$C_{p,q}^{i,j}(n) = X_{i,j}(n) * X_{p,q}(n) = \sum_{k=0}^{L-1} X_{i,j}(k) X_{p,q}(n-k) \quad (2)$$

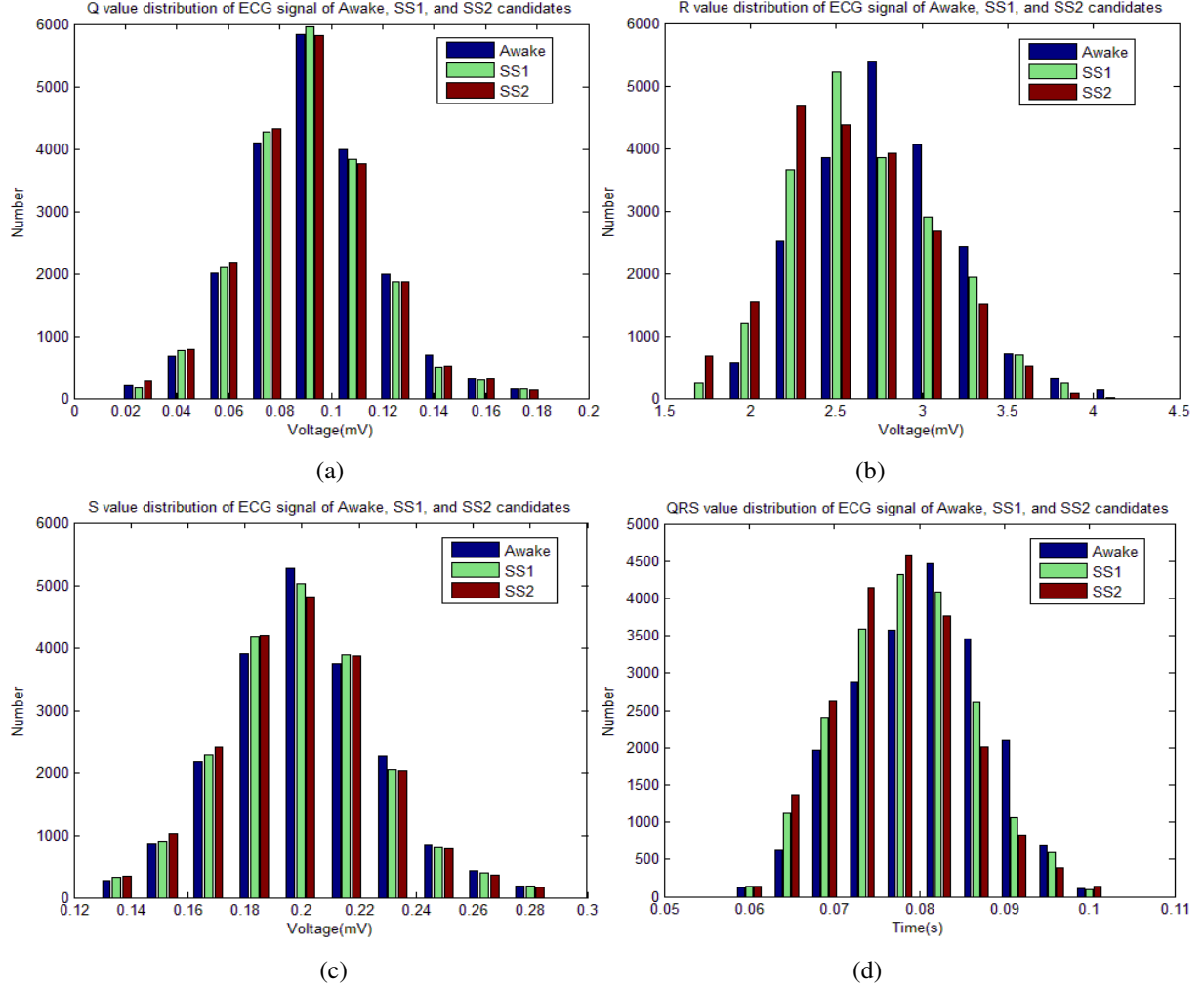


Fig. 4. Distributions of various values of the ECG frame. (a) Distribution of the value of the Q wave. (b) Distribution of the value of the R wave. (c) Distribution of the value of the S wave. (d) Distribution of the duration of the QRS complex.

It is worth noting that the cross correlation is related to the convolution by the following relationship:

$$R_{p,q}^{i,j}(n) = X_{i,j}(n) * X_{p,q}(-n) \quad (3)$$

In the following, the convolution and the cross correlation are referred as the correlation analysis. The correlation analysis measures the similarity of every pair of ECG signals $X_{i,j}(n)$ and $X_{p,q}(n)$. This information is used to form the kernel for performing the drowsiness detection. The problem is formulated as a multi-objective optimization problem and the solution of the optimization problem is found by a genetic algorithm. Section IV B will discuss why both $C_{p,q}^{i,j}(m)$ and $R_{p,q}^{i,j}(m)$ are employed for the design of the kernel. The convolution based kernel matrix $K_{conv,ij}$ and the cross correlation based kernel matrix $K_{corr,ij}$ found by the genetic algorithm are denoted as:

$$K_{conv,ij} = \begin{bmatrix} X_{conv,1,1} & \cdots & X_{conv,1,N_t} \\ \vdots & \ddots & \vdots \\ X_{conv,N_t,1} & \cdots & X_{conv,N_t,N_t} \end{bmatrix} \quad (4)$$

and

$$K_{corr,ij} = \begin{bmatrix} X_{corr,1,1} & \cdots & X_{corr,1,N_t} \\ \vdots & \ddots & \vdots \\ X_{corr,N_t,1} & \cdots & X_{corr,N_t,N_t} \end{bmatrix} \quad (5)$$

where $N_t=54000$ which is 90% of the total number of training data points in the dataset. A conventional 10-fold cross validation method is employed for the training and the testing [31]. Firstly, the ECG dataset is divided into 10 sets randomly. Each set contains 6000 samples which are 10% of the total number of training data points in the datasets. Here, there are 2000 samples for every class. 9 sets of data is used for the training and the remaining 1 set of data is used for the validation. This process completes one fold of operations. Now, another set is chosen for the validation and the rest 9 sets are used for the training. It is worth noting that that this chosen validation set is different from the validation sets chosen in previous folds of operations. This fold of operations is repeated until all these 10 sets are validated. Here, $X_{conv,a,b}$ and $X_{corr,a,b}$ are defined as:

$$X_{conv,a,b} = \sum_{m=1}^{2L-1} \omega_{conv,ij,m} C_{p,q}^{i,j}(m) \quad (6)$$

and

$$X_{xcorr,a,b} = \sum_{m=1}^{2L-1} \omega_{xcorr,ij,m} R_{p,q}^{i,j}(m) \quad (7)$$

where $X_{conv,a,b}$ and $X_{xcorr,a,b}$ are the convolution sum and the cross correlation sum of the ECG signal a and the ECG signal b , respectively. Here the starting time index of the convolution and the cross correlation of the first signal $X_{0,1}(n)$ is 1 and the ending time index of the convolution and the cross correlation of the second signal $X_{2,20000}(n)$ is 60000. In general, the kernel affects predominantly the maximum margin and the overall accuracy of the DDC. It can be seen from (4) and (5) that the maximum margin is directly related to both $X_{conv,a,b}$ and $X_{xcorr,a,b}$. Based on (6) and (7), an optimal design of both $X_{conv,a,b}$ and $X_{xcorr,a,b}$ can be obtained by an optimal design of the corresponding weighting factors, namely, $\omega_{conv,ij,m}$ and $\omega_{xcorr,ij,m}$ for $m = 1, 2, \dots, 2L - 1$, for the given sequences of $C_{p,q}^{i,j}(m)$ and $R_{p,q}^{i,j}(m)$, respectively. In general, an optimally designed kernel will speed up the convergence of the training algorithm. However, different combinations of $\omega_{conv,ij,m}$ and $\omega_{xcorr,ij,m}$ will come up with different kernels. Finding the optimal weight requires a huge computational power. Thus, there is a tradeoff between the affordable computational power based on the rate of the convergence of the training algorithm and the acceptable accuracy. Since it is very difficult to find the optimal value of $\omega_{conv,ij,m}$ and $\omega_{xcorr,ij,m}$ due to the complexity of the objective function, a good trial of $\omega_{conv,ij,m}$ and $\omega_{xcorr,ij,m}$ are primary important which determines the overall accuracy.

In this paper, an optimization approach is employed to determine the weighting factors $\omega_{conv,ij,m}$ and $\omega_{xcorr,ij,m}$. However, exhaustive search algorithms may not be the appropriate choices for finding the solution of the optimization problem. This is because it deals with a huge of combinations. In general, heuristic search algorithms perform the searching of the optimal solutions efficiently and effectively. In particular, the genetic algorithm is a robust searching heuristic algorithm which imitates the process of the natural evolution for searching the solution of the optimization problem by the inheritance, mutation, selection and crossover operations.

The Mercer kernels or the inner product kernels $K_{conv,ij}$ and $K_{xcorr,ij}$ obey the Mercer theorem. Thus, the Mercer kernels satisfy the symmetric and positive semi-definite requirements [32]. The eigenvalues of $K_{conv,ij}$ and $K_{xcorr,ij}$ can be evaluated as follows:

$$\begin{cases} K_{conv,ij} V_{conv} = D_{conv} V_{conv} \\ K_{xcorr,ij} V_{xcorr} = D_{xcorr} V_{xcorr} \end{cases} \quad (8)$$

where V_{conv} and V_{xcorr} are the nonzero eigenvectors as well as D_{conv} and D_{xcorr} are the corresponding eigenvalues. D_{conv} and D_{xcorr} can be evaluated such that all the eigenvalues are positive. This ensures that $K_{conv,ij}$ and $K_{xcorr,ij}$ are positive semi-definite. Thus, the kernel may map the ECG signals in the Euclidean space to another Hilbert space which facilitates the drowsiness detection [32].

In this investigation, the properties including the maximum margin and the overall accuracy (OA) are considered. In principle, when more than one objective is considered, the problem is a multi-objective optimization problem [33]. There is an efficient algorithm for finding the optimal solutions of the optimization problem with fast convergences. Hence, multi-objective optimization algorithms have a tremendous practical importance since most real world optimization problems may ideally consist of multiple conflicting objectives [30]. In the design of the pre-computed kernel of DDC (K_{DDC}), the weighting factors $\omega_{conv,ij,m}$ and $\omega_{xcorr,ij,m}$ are evaluated.

Here, an optimal design of the K_{DDC} based on the convolution and the cross correlation of the ECG signals is formulated as a multi-objective optimization problem. The multidimensional space of the objective functional values is known as the objective space [34]. In this paper, a genetic algorithm is employed for finding the solution of the multi-objective optimization problem [30]. This algorithm provides a good tradeoff between the required computational power and the accuracy of the solution. The algorithms for the optimal design of the kernel functions are shown in Fig. 5. In particular, the detailed procedures in terms of the pseudo codes are shown. Firstly, the size of the population and the initial objective functional values are initialized. The objective functional values of the individuals in the population will be computed based on the initial objective functional values. The rank of the individuals is assigned based on the objective functional values. It is worth noting that the convergence of the population is mainly dependent on a small group of the pareto optimal solutions instead of all the optimal solutions because of the nature of the stochastic selection errors in a finite population size. Niche count is applied to increase the diversity of the population by increasing the distance between two solutions on the axis of the objective functions [30]. Hence, the convergence of the small group solutions can be avoided. Afterwards, the genetic operations will be implemented to generate a new offspring and the objective functional value will be evaluated. Also, the rank assignment as well as the niche count will be computed repeatedly on the new offspring. The genetic algorithm will be terminated until it reaches the maximum number of generations and the output reaches the pareto front which is the set of the optimal non-dominated solutions.

Define K_{DDC} as the sum of $K_{conv,ij}$ and $K_{xcorr,ij}$. It is proved below that the K_{DDC} is also a Mercer kernel [32]. From (8), if $K_{conv,ij}$ and $K_{xcorr,ij}$ are positive semi-definite, then for any $c \in \mathfrak{R}^n$, $c^T K_{conv,ij} c \geq 0$ and $c^T K_{xcorr,ij} c \geq 0$. Hence, we have

$$\begin{aligned} c^T K_{DDC} c &= c^T (K_{conv,ij} + K_{xcorr,ij}) c \\ &= c^T K_{conv,ij} c + c^T K_{xcorr,ij} c \end{aligned} \quad (9)$$

Therefore, the K_{DDC} is also a positive semi-definite kernel. Thus, it is a Mercer kernel.

The rationale for the construction of the K_{DDC} is to exploit the advantages of both $K_{conv,ij}$ and $K_{xcorr,ij}$. Thus, the overall accuracy of the DDC is improved. Now, two objective functions are defined as follows:

$$\begin{aligned} \text{Max } F_1 &= \tilde{M}(\alpha, \omega) \\ \text{Max } F_2 &= OA \end{aligned} \quad (10)$$

$$\text{s.t. } \begin{cases} \alpha_i \geq 0, \sum_{i=1}^N \alpha_i y_i = 0, \text{ with } i = 1, \dots, N. \\ \sum_{n=1}^{2L-1} \omega_{conv,ij,n} = 1, \sum_{n=1}^{2L-1} \omega_{xcorr,ij,n} = 1 \end{cases} \quad (11)$$

where α_i is the Lagrange multiplier and $y_i \in \{-1, +1\}$ is the output of the classifier. Also, $\tilde{M}(\alpha, \omega)$ is the maximum margin function of the K_{DDC} for training these three classifiers based on the support vector machine. These three classifiers are denoted as C0 for classifying the awake stage and the sleep stage 1, C1 for classifying the awake stage and sleep stage 2, and C2 for classifying the sleep stage 1 and the sleep stage 2.

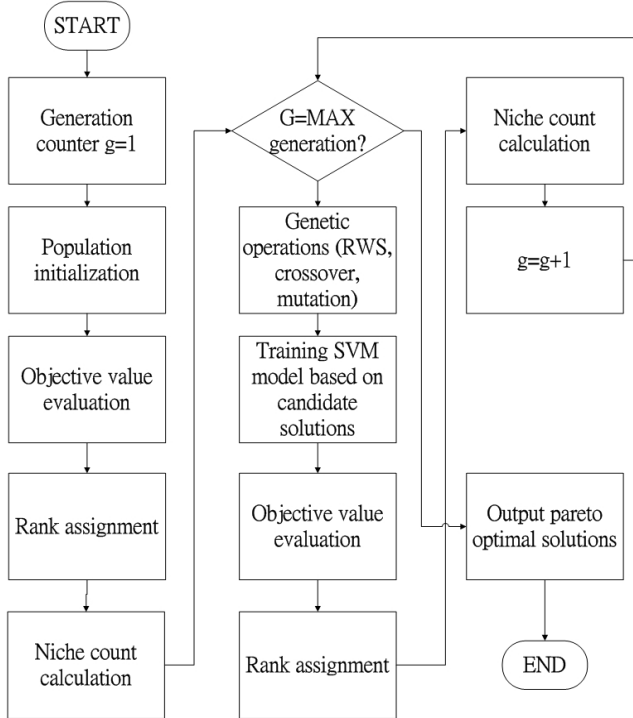


Fig. 5. Flow chart of the optimal design of the kernel function.

In this paper, $\omega_{conv,ij,m}$ and $\omega_{xcorr,ij,m}$ are the variables that affect F_1 and F_2 . They are obtained using the multi-objective based genetic algorithm (MOGA). In the MOGA, two objectives, namely F_1 and F_2 , are considered. They are the maximum margin function and the overall accuracy,

respectively. The obtained pareto front contains the optimal solutions of $\omega_{conv,ij,m}$ and $\omega_{xcorr,ij,m}$ based on the objective functions F_1 and F_2 . $R_{p,q}^{i,j}(n)$ captures the symmetric information among the ECG signals from different classes. $C_{p,q}^{i,j}(n)$ captures the anti-symmetric information among the ECG signals from same class. The components contain both the symmetric and the anti-symmetric information. The margin function of the maximum margin classifier is given by [28]:

$$\tilde{M}(\alpha, \omega) = \sum_{i=1}^N \alpha_i - \frac{1}{2} \sum_{i=1}^N \sum_{j=1}^N \alpha_i \alpha_j y_i y_j K_{DDC} \quad (12)$$

K_{DDC} captures all representative characteristics of the awake stage, the sleep stage 1 and the sleep stage 2. Thus, the DDC achieves an accurate result for the drowsiness detection. The multi-objective optimization based genetic algorithm will carry out the mutation for generating a new trial for the optimization until the optimal K_{DDC} is obtained.

The Overall Accuracy, OA, is related to the sensitivity S_e and the specificity S_p as follows [31]:

$$OA = 0.5(S_e + S_p) \quad (13)$$

where the sensitivity is the true positive rate and the specificity is the true negative rate. They are defined as follows:

$$S_e = \frac{TP}{TP + FN} \quad (14)$$

and

$$S_p = \frac{TN}{TN + FP} \quad (15)$$

where TP is the total number of the true positive, FN is the total number of the false negative, TN is the total number of the true negative and FP is the total number of the false positive of the testing points.

Thus, the optimal tradeoff solutions can be obtained by performing the MOGA with the above objective functions.

The pseudo code has been provided to better assist the understanding of the proposed algorithm.

IV. COMPARISONS AND PERFORMANCE EVALUATIONS OF DDC

Section IV is divided into four sub-sections. In section IV A, the feature extraction using numerous prevailing typical kernels is performed. The best prevailing kernel for an application of the DDC will be discussed. In section IV B, OA, S_e and S_p of $K_{xcorr,ij}$ and $K_{conv,ij}$ are evaluated and compared to that of K_{DDC} . It will be demonstrated that the K_{DDC} achieves the most accurate result since it exploits the advantages of both $K_{conv,ij}$ and $K_{xcorr,ij}$. In section IV C, the accuracy and the measurement stability of our proposed method are compared to that of the related works. Finally, a testing study on the drowsiness detection system based on the K_{DDC} will be presented in section IV D.

A. Final Stage

To demonstrate the effectiveness of the developed kernel, the performance of the prevailing kernels for the feature extraction

is compared. In this section, the features are obtained from the convolution and cross correlation. The lengths of the feature vectors are equal to $2L-1$. The typical kernels employed in this paper for the comparison include the linear, quadratic, third order polynomial and Gaussian radial basis function. The feature extraction based on these typical kernels is performed. A combination of different scenarios is then evaluated. A 10 fold cross validation is used for the performance evaluation of the kernels [31]. The classifiers are deduced using the 1-against-1 multi-class SVM. This is because the 1-against-1 multi-class SVM approach was proved to be better than the 1-against-all multi-class SVM [35]. In this investigation, an optimization approach is not employed. The OA, S_e and S_p of each scenario will be evaluated.

Algorithm 1

Data: ECG datasets retrieved from 126 candidates [26], X_m

Loop from $m=1:126$

$X_{i,j} \leftarrow \text{BeatSegmentation}(X_m)$

End loop

Divide 60000 ECG frames randomly into 10 equal-sized subsets; each set contains 6000 (10%) samples in which each class contributes 2000 samples;

Repeat

Pick 9 subsets as training datasets and the remaining 1 subset as validation datasets;

The validation datasets cannot be reused for validation;

Loop from $i=0:2$

Loop from $j=1:20000$

Loop from $p=0:2$

Loop from $q=1:20000$

$R_{p,q}^{i,j}(k) \leftarrow \text{CrossCorrelation } X_{i,j} \& X_{p,q}$

$C_{p,q}^{i,j}(k) \leftarrow \text{Convolution } X_{i,j} \& X_{p,q}$

End loop

End loop

End loop

End loop

Construct cross-correlation kernel 54000×54000 $K_{\text{xcorr},ij}$. The entry (a,b) of $K_{\text{xcorr},ij}$ is defined as the weighting sum of cross-correlation coefficients $R_{p,q}^{i,j}(k)$ between signal a and signal b;

Construct convolution kernel 54000×54000 $K_{\text{conv},ij}$. The entry (a,b) of $K_{\text{conv},ij}$ is defined as the weighting sum of convolution-correlation coefficients $C_{p,q}^{i,j}(k)$ between signal a and signal b;

$\text{Model} \leftarrow \text{TrainClassifier}(\text{Classlabel}, K_{\text{xcorr},ij}, K_{\text{conv},ij})$

Construct cross-correlation testing kernel 6000×6000 $\text{test}K_{\text{xcorr},ij}$. The entry (a,b) of $\text{test}K_{\text{xcorr},ij}$ is defined as the weighting sum of cross-correlation coefficients $R_{p,q}^{i,j}(k)$ between signal a and signal b;

Construct convolution testing kernel 6000×6000 $\text{test}K_{\text{conv},ij}$.

The entry (a,b) of $\text{test}K_{\text{conv},ij}$ is defined as the weighting sum of convolution-correlation coefficients $C_{p,q}^{i,j}(k)$ between signal a and signal b;

$(OA, S_e, S_p, EA) \leftarrow$

$\text{TestClassifier}(\text{model}, \text{test}K_{\text{xcorr},ij}, \text{test}K_{\text{conv},ij})$

End repeat until all validation datasets have been utilized

Algorithm 2 *BeatSegmentation* (X_m)

Data: ECG datasets retrieved from 126 candidates [26], X_m

Output: ECG frames $X_{i,j}$

Step 1: Filter X_m using low pass filter H_{low} and derivative filter H_d ;

Step 2: Square the signal and carry out moving window integration;

Step 3: Locate Q and S waves based on the output of moving window integration;

Step 4: Locate R waves (peak between Q and S waves);

$X_{i,j}$ ($i=0,1,2=\text{class label}, j=1,\dots,20000$) \leftarrow Portion of signal between consecutive R waves;

Algorithm 3

$\text{TrainClassifier}(\text{Classlabel}, K_{\text{xcorr},ij}, K_{\text{conv},ij})$

Data: Classlabel, $K_{\text{xcorr},ij}$, $K_{\text{conv},ij}$

Output: Model

Step 1: generations = 1

Step 2: initialization (population)

Step 3: Evaluate the individuals with the fitness function (F1 and F2)

Step 4: rank the individuals by their fitness values by step 3

Step 5: do the Niche count calculation

while generations \leq max_generation **do**

Step 6: Select two parents from the population

Step 7: Create the offspring using Roulette wheel selection , crossover and mutation

Step 8: train SVM model for each individual

Step 9: Evaluate the offspring with the fitness function (F1 and F2)

Step 10: rank the individuals by their fitness values by step 3

Step 11: do the Niche count calculation

Step 12: Decide the new population based on the offspring

Step 13: generations = generations + 1

End while

Model \leftarrow Pareto solutions

The plots of the overall accuracies based on the cross correlation features (Xcorr) and the convolution features (Conv) against the feature vector dimensions (D) are shown in Fig. 6a and Fig. 6b, respectively. In addition, the plot of the sum of the cross correlation and the convolution (Xcorr+Conv) against D is shown in Fig. 6c. It is worth noting that there are 199 scenarios for the results plot in each curve in Fig. 6.

The best scenario of each of twelve simulated curves shown

in Fig. 6 is plotted in Fig. 7. The performance of the classifier based on OA of the best scenario under three possible feature extraction choices, namely, Xcorr, Conv and Xcorr+Conv is demonstrated. Here, the linear kernel function is used. It can be seen that the hybrid feature extraction approach, Xcorr+Conv, achieves the best performance in terms of OA compared to those of the Xcorr approach and the Conv approach. The obtained OA are between 59.36% and 66.73%.

The feature extraction approach based on the quadratic kernel function achieves OA between 65.93% and 69.54%. It is worth noting that no significant improvement is achieved compared to that of the linear kernel function.

For the third order polynomial kernel function, the classifier achieves the OA between 69.41% and 76.93%. Among these three feature extraction approaches, the Xcorr approach achieves the similar OA performance compared to the Xcorr+Conv approach. The difference between these two approaches is only 0.12%.

The last result is based on the RBF kernel function. The classifiers based on the Xcorr, Conv and Xcorr+Conv approaches yield the OA of 72.31%, 78.62% and 82.84%, respectively.

Among the aforementioned four prevailing kernel functions, the classifier based on the RBF kernel function yields the best performance compared to the third order polynomial function, the quadratic kernel function and the linear kernel function. However, the maximum OA is only 82.84%. These prevailing kernel functions are far to be acceptable for practical applications because the OA should be greater than 95% for practical uses.

B. Comparison to Various Classifier

In this section, the performance of kernels $K_{\text{Xcorr},ij}$, $K_{\text{Conv},ij}$ and K_{DDC} are compared. A 10-fold cross validation is employed for the verification [31]. The OA, Se and Sp of $K_{\text{Xcorr},ij}$ are 87.38%, 87.49% 87.27%, respectively. Those of $K_{\text{Conv},ij}$ are 84.76% 85.09% 84.43%, respectively. Those of K_{DDC} are 97.01%, 97.16% 96.86%, respectively. Thus, it can be seen that the proposed K_{DDC} meets the requirement of having error less than 5%.

Fig. 8 shows the comparisons of the performances of K_{DDC} to those of the classifier 0, classifier 1 and classifier 2. The results reveal that the OA, S_e and S_p of K_{DDC} outperform those of the typical kernels by 17% to 63%. Intuitively, K_{DDC} adaptively customizes the kernel to this specific drowsiness detection application. Also, the convolution kernel captures the anti-symmetric information among the ECG signals from the same class whereas the cross correlation kernel captures the symmetric information among the ECG signals from different classes. As the K_{DDC} captures both the symmetric and anti-symmetric information, it can achieve a better performance than using either one kernel. In contrast to the typical kernels such as the linear, quadratic, polynomial and Gaussian radial basis function, they are not designed for particular applications.

Denote the performance of the i^{th} kernel as $P(i)$. Denote $P(i)_{j,k,l}$ as the average performance of the i^{th} kernel processed by

the indicators j,k,l . Here, $P(i)_{j,k,l} > P(i_2)_{j,k,l}$ means that the average score of the i_1^{th} kernel processed by the indicators j,k,l is higher than the average score of the i_2^{th} kernel processed by the indicators j,k,l . From Fig. 8, it can be seen that $P(K_{\text{DDC}}) > P(K_{\text{Xcorr},ij}) > P(K_{\text{Conv},ij})$. Also, $P(K_{\text{DDC}})_{OA, Se, Sp}$ is better than $P(K_{\text{Xcorr},ij})_{OA, Se, Sp}$ by 11%. Moreover, $P(K_{\text{DDC}})_{OA, Se, Sp}$ is better than $P(K_{\text{Conv},ij})_{OA, Se, Sp}$ by 14%. This implies that the K_{DDC} achieves the highest OA, S_e and S_p . The superiority of K_{DDC} over $K_{\text{Xcorr},ij}$ and $K_{\text{Conv},ij}$ is attributed to the fact that K_{DDC} takes the advantages of both $K_{\text{Xcorr},ij}$ and $K_{\text{Conv},ij}$. Finally, it can be seen that the K_{DDC} is an optimal design.

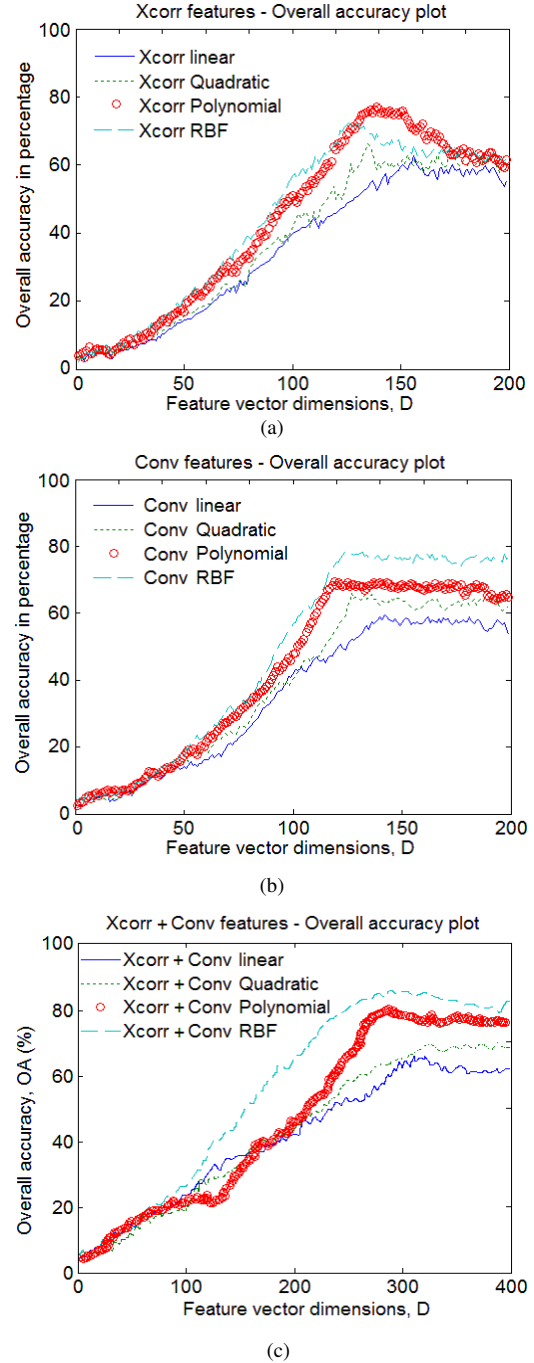


Fig. 6. Overall accuracy based on different kernel functions. (a) Cross correlation features. (b) Convolution features. (c) Cross correlation and convolution features.

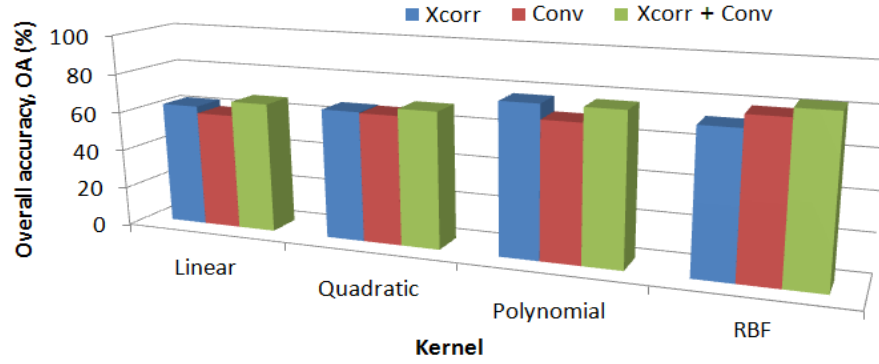


Fig. 7. Performance of the best scenario under different feature extraction kernels.

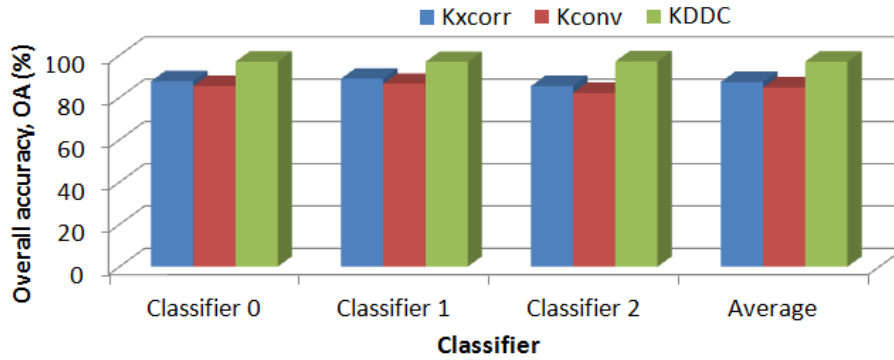


Fig. 8. Comparison on the overall accuracy of the pre-computed kernel based classifier.

C. Comparisons to Related Works

The measurement stability (MS) is defined as the time ratio that a signal can be measured successfully. For instance, for a measurement of a signal with the duration 10s, MS=50% means that a total of 5s has been distorted. This leads to an error in the feature extraction. Thus, it results to making an incorrect decision. The motion artifacts due to the movements and the friction between the electrodes and the human body [16] are the main reason of the distortions of the EEG and the ECG. As the classifier cannot yield the correct output for the distorted signal, the instant warning cannot be provided to the drowsy driver. Thus, a parameter, namely the equivalent accuracy (EA), is defined as follow to reflect the accuracy of the classifier:

$$EA = OA \cdot MS \quad (16)$$

Most existing works are based on the simulation results performed on the driving datasets [6], [9], [11], [13], [14]. However, this is not sufficient for reflecting the driver's condition. In contrast, our developed K_{DDC} adopts the real world ECG signal which accurately extracts the "sleepiness" characteristics and the status of the drivers. It is worth noting that the dataset in [9] was obtained by the car simulation game with the data captured by the camera together with the vehicle data logger. On the average, the OA can reach up to 90% [9]. However, the driving simulation tools cannot simulate the potential risks since the drivers will never experience any accident based on the simulation tools. Thus, the driving datasets based on the simulation cannot reflect the real situation. For the occurrence of the negative response, the real world experimental results and the simulation results based on the driving datasets are not consistent. Besides, the experimental data in [14] were analyzed via six participants with their EEG

signals obtained by the EEG/EOG electrodes. A neural fuzzy system is employed for classifying the sleep levels. The average IA can only achieve 69%, which is much lower than that of our K_{DDC} .

Table II summarizes the performance of various methods. It can be seen that the image based methods achieve the overall accuracies of 89% [5], 86% [6] and 94.84% [8]. However, these methods assumed a perfect detection of the eyes and pupils. Indeed, this is not the practical situation. In the practical situation, the MS is 58.75% [16]. Thus, the EA does not exceed 60%. For the vehicle based methods, the overall accuracies of 90% [9] and 67% [11] were achieved for the drowsiness detection. However, there is a bias and the performance evaluation is insufficient in [9]. This is because there is no cross validation. One can pick up a bias training dataset to train the classifier. As the vehicle based features are not directly related to the human behaviors and the sleepiness, the former investigation based on the biometric signals achieves the overall accuracies of 69% [13] and 75% [14] when the EEG and the EOG signals are used. Although the method based on the biometric signals has a MS of 85%, the resultant EA is much lower than that of our proposed K_{DDC} . The reason for the EEG based method achieving the low accuracy is that the collected EEG signal is severely influenced by the psychological status. As the psychological status of the driver is arbitrary and varies from time to time, there is no standard threshold for the detection. Besides, the EOG sensor is different from the EEG and the ECG sensors. They are not exactly stuck on the driver. The sensing interface is extremely unstable due to many human activities. Hence, the collected EOG signal is unreliable and a low accuracy is achieved.

TABLE II. PERFORMANCE COMPARISON OF PROPOSED AND RELATED WORKS

Drowsiness Algorithms	Drowsiness measure	Sensors requirement	Datasets	OA	Se	Sp	MS [22]	EA
Viola-Jones and CART method [5]	Image-based – Eye blinking	Camera	2500 image frames	89%	N/A	N/A	58.75%	52.29%
Active shape model [6]	Image-based – Eye movement	Camera	Moving base driving simulator - 225 awake samples, 181 drowsy samples, 158 very drowsy samples	86%	N/A	N/A	58.75%	50.53%
Support Vector Machine with features of eye index, pupil activity and head pose [8]	Image-based – Eye movement and head pose	Camera	5 participants with 75 video segments (each segment is 4s long), frame rate of 30 frames/s	94.84%	N/A	N/A	58.75%	55.72%
Support Vector Machine with steering angle and distance to outside lane analysis using radial basis function [9]	Vehicle-based – steering angle and distance to outside lane	Camera and vehicle data logger	GTR car simulation game – 10 participants play at day time 11:00-13:00 and at mid-night 01:00-03:00	90% (1-fold validation)	N/A	N/A	N/A	N/A
Both laboratory-based and high-fidelity driving simulator studies [11]	Vehicle based-Physical examinations, blood chemistry and questionnaire	High-fidelity driving simulator	12 participants in day time and 29 participants in night time	67%	N/A	N/A	N/A	N/A
Self-organizing Neural Fuzzy System [13]	Biometric signal – EEG	33 Ag/AgCl EEG/EOG electrodes	6 participants using Virtual Reality based dynamic driving simulator (total of 1594 samples)	69%	N/A	N/A	85%	58.65%
Independent component analysis with reference for electrooculography artefacts removal [14]	Biometric signal - EEG	Fz-A1, Cz-A2, and Oz-Pz EEG channels	40 participants using third generation moving base driving simulator (260 samples)	75%	86%	64%	85%	63.75%
Support Vector Machine with precomputed kernel via optimal correlation analysis [Proposed]	Biometric signal – ECG signal	ECG sensor	20000 samples in each of driving candidate, stage 1 sleep candidate and stage 2 sleep candidate	97.01% (10-fold cross validation)	97.16%	96.86%	97.5%	94.58%

For practical applications, the EA is considered as the essential parameter to determine the true accuracy of the driver drowsiness detection. It can be seen that the proposed K_{DDC} achieves an outstanding performance of EA=94.58%. Here, the measurement instability is less than 5%. That is, MS=97.5% [16]. It improves the performance from 48.4% $(0.9458-0.6375)/0.6375 \times 100\% = 48.4\%$ to 87.2% $(0.9458-0.5053)/0.5053 \times 100\% = 87.2\%$ when compared to the related works [5], [6], [8], [13], [14]. In addition, our proposed K_{DDC} achieves the highest EA even though the MS is assumed to be 100% in [9], [11], [15].

There are several reasons why our proposed method achieves the highest EA. First, the MS is the highest compared to the EEG based method and the image based method. Also, the drowsiness is not the unique reason for the blinking. Hence, monitoring the frequency of blinking may not capture the essential features for constructing a DDC. Regarding to the OA=69% [13] and the OA=75% [14] achieved by the EEG based method, the reasons for not achieving the satisfactory performance is due to the redundant and the misleading features added to the classifier. Another potential reason is that more important and representative features have not been extracted.

For our proposed support vector machine with the

pre-computed kernel designed by the optimal correlation analysis, the kernel K_{DDC} has been adaptively customized the driver drowsiness detection. Also, the design optimally captures both the symmetric and the anti-symmetric information for distinguishing among the awake stage, the sleep stage 1 and the sleep stage 2. Thus, an excellent performance is achieved.

D. Testing the Drowsiness Detection System

The simulation results have been presented in the previous sections. In this subsection, a prototype for the driver drowsiness detection system is built. The performance evaluation including a latency study is illustrated. Fig. 9 shows the flow chart for performing the performance evaluation of the system. The steps for performing the latency study are similar to that for performing the simulations except the ECG module and an arbitrary waveform generator are employed for the testing purpose. A 10-fold cross validation is employed for evaluating the classifier. The fold index $I=1$ is initialized. The terminating condition of $I>10$ is checked. 90% of the signals in the normal driving ECG dataset and 90% of the signals in the drowsy ECG dataset are randomly selected for the construction of the training dataset. The data processing operations are applied to all training signals. Then, the training of the driver drowsiness classifier is carried out. The trained classifier is programmed

into an ECG module. The remaining 10% of signals in the normal driving ECG dataset and the remaining 10% signals in the drowsy ECG dataset are employed as the testing signals. Signals generated by an arbitrary waveform generator are also loaded into the testing dataset. The signals in this testing dataset will be fed into the ECG module. The evaluation parameters, OA, Se, Sp and the delay are recorded. These processes are repeated until all 10-folds have been validated.

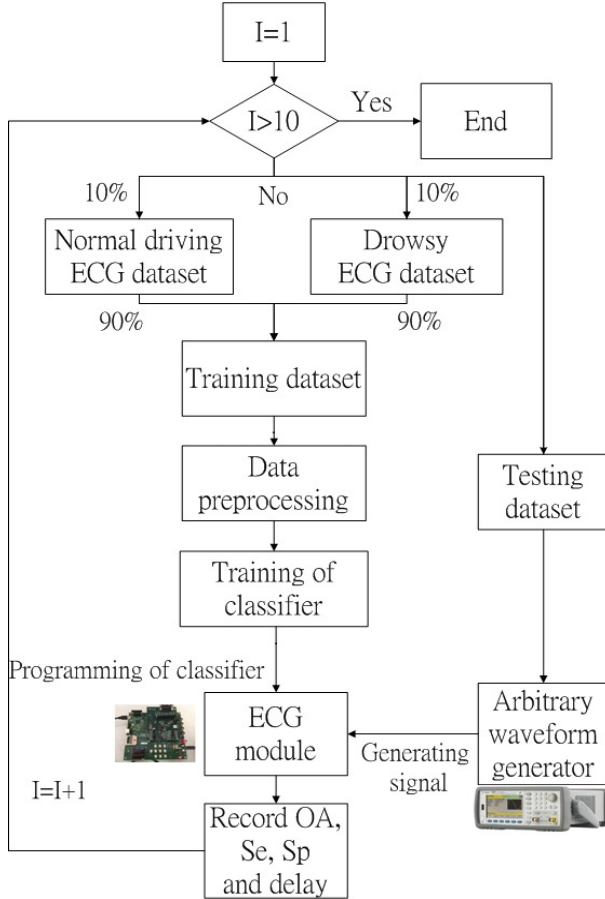


Fig. 9. Flow chart for performing the performance evaluation of the driver drowsiness system.

Fig. 10 shows the comparison results on the overall accuracies of K_{DDC} (simulation) to those of K_{DDC} (testing). It can be seen that the K_{DDC} (testing) achieves the average OA of 96.78%. It is less than 1% of the simulated data. This small discrepancy (<1%) is due to the imperfect generation of the ECG signal by the arbitrary waveform generator.

Fig. 11 shows the results on the latency delay of the driver drowsiness system. The average delay is defined as follows. 40000 samples are validated in the 10-fold cross validation for each classifier. The delay between the received signal generated by the arbitrary waveform generator and the decision output at the ECG module is recorded for every sample. In particular, a C program is written for calling a timer function of the MCU program of the ECG module. It determines how fast the DDC returns before the timer expire. If the timer expires in T microseconds and the DDC call returns N times during this interval, then the delay behind a DDC call is T/N microseconds. The delay for each sample is obtained and the 40000 delays are

averaged for computing the average delay. In Fig. 11, the average delay of the ECG signals of each classifier is demonstrated. In particular, it is found that the average delays of the Classifier 0, the Classifier 1 and the Classifier 2 are 0.534ms, 0.549ms and 0.54ms, respectively. Note that the total delays are the sum of delays of any two classifiers (~1ms). The small latency (~1ms) reveals that the proposed system can be applied to this real time monitoring and classification drowsiness detection system.

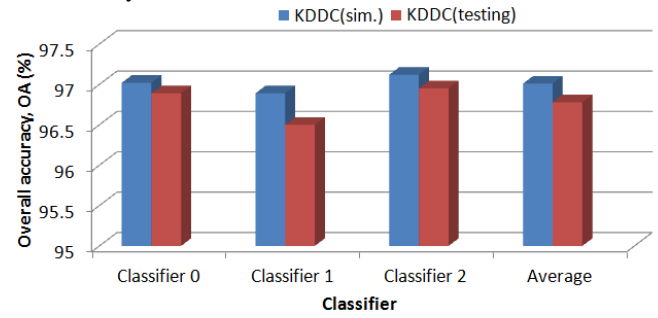


Fig. 10. Comparison of the overall accuracy of the K_{DDC} (sim.) to K_{DDC} (Testing).

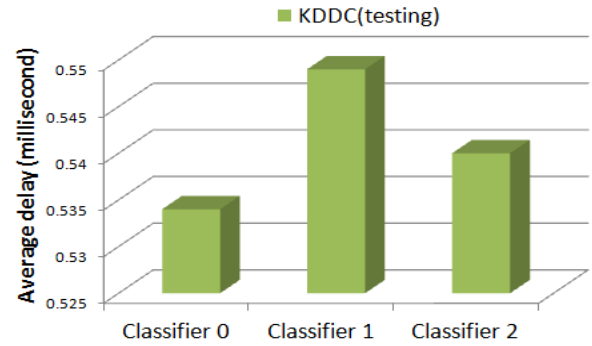


Fig. 11. Average delay of K_{DDC} (Testing).

V. CONCLUSION

In this paper, a driver drowsiness classifier (DDC) based on the ECG signals is developed. Also, a self defined kernel is designed and implemented based on the optimal correlation analysis. The convolution kernel is fused with the cross correlation kernel by a genetic algorithm. In the performance evaluation, the DDC obtains an overall accuracy of 97.01%, the sensitivity of 97.16% and the specificity of 96.86%. If either the convolution or the cross correlation kernel is employed, then the performance of the classifier will be degraded by more than 10% on average. The comparison results reveal that the performance is downgraded by 17% to 63% if the feature selection is performed by the typical kernels. It can be seen that the driver drowsiness detection via the ECG signals outperforms those based on the existing methods. Due to the high measurement stability and the high immunity to noise of the ECG signals compared to the image based EEG and EOG signals, the ECG signals find more important applications in the market. Also, our proposed kernel improves the performance by 48.4% to 87.2% compared to related image based methods and

the biometric signal based methods.

$K_{\text{corr},ij}$ captures the symmetric information among the ECG signals from different classes whereas $K_{\text{conv},ij}$ captures the anti-symmetric information among the ECG signals from the same class. Hence, the K_{DDC} can achieve a better performance than the prevailing kernels. This is because both the symmetric and anti-symmetric information of the ECG signals are highly related to the three driver states, namely the awake stage, the sleep stage 1 and the sleep stage 2. Also, the K_{DDC} is adaptively designed and customized to the driver drowsiness detection application.

It is found that the testing results are 99% close to the simulated results. On the other hand, the average delays of the Classifier 0, the Classifier 1 and the Classifier 2 are 0.534ms, 0.549ms and 0.54ms, respectively. Hence, the required computational power of the system is low enough for the *real time* application.

From the statistical viewpoint, 97% of the accidents are caused by the drowsy drivers. Hence, if the developed DDC is fully utilized in the world wide market, then 1.26 million people may be rescued and 48.5 million traffic injuries may be avoided [1]. This also saves more than 500 billion USD in the medical expenses.

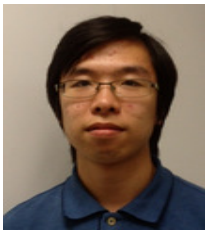
ACKNOWLEDGMENT

The support from the Wireless Sustainability Center of the Department of Electronic Engineering, City University of Hong Kong is gratefully acknowledged.

REFERENCES

- [1] *Global status report on road safety 2013*, World Health Organization., Geneva, Switzerland, 2013.
- [2] K. Dalal, Z. Lin, M. Gifford, and L. Svanström, "Economics of global burden of road traffic injuries and their relationship with health system variables," *Int. J. Prev. Med.*, vol. 4, no. 12, pp. 1442-1450, Dec. 2013.
- [3] *Drowsy driving and automobile crashes*, National Highway Traffic Safety Administration., 2012.
- [4] M. R. Rosekind, "Underestimating the societal costs of impaired alertness:safety, health and productivity risks," *Sleep Medicine*, vol. 6, pp. S21-S25, Jun. 2005.
- [5] R. Ahmad, and J. N. Borole, "Drowsy Driver Identification Using Eye Blink Detection," *IJISSET - International Journal of Computer Science and Information Technologies*, vol. 6, no. 1, pp. 270-274, Jan. 2015.
- [6] W. Zhang, B. Cheng, and Y. Lin, "Driver drowsiness recognition based on computer vision technology," *Tsinghua Science and Technology*, vol. 17, no. 3, pp. 354-362, Jun. 2012.
- [7] V. K. Diddi, and S. B. Jamge, "Head Pose and Eye State Monitoring (HEM) for Driver Drowsiness Detection: Overview," *IJISSET - International Journal of Innovative Science, Engineering & Technology*, vol. 1, no. 9, pp. 504-508, Nov. 2014.
- [8] R. O. Mbouna, S. G. Kong, and M. -G. Chun, "Visual Analysis of Eye State and Head Pose for Driver Alertness Monitoring," *IEEE Trans. Intell. Transp. Syst.*, vol. 14, no. 3, pp. 1462-1469, Sep. 2013.
- [9] A. Abas, J. Mellor, and X. Chen, "Non-intrusive drowsiness detection by employing Support Vector Machine," *2014 20th International Conference on Automation and Computing (ICAC)*, Bedfordshire, UK, 2014, pp. 188-193.
- [10] A. Sahayadhas, K. Sundaraj, and M. Murugappan, "Detecting driver drowsiness based on sensors: a review," *Sensors*, vol. 12, no. 12, pp. 12937-12953, Dec. 2012.
- [11] P. M. Forsman, B. J. Vila, R. A. Short, C. G. Mott, and H. P. A. V. Dongen, "Efficient driver drowsiness detection at moderate levels of drowsiness," *Accident Analysis & Prevention*, vol. 50, pp. 341-350, Jan. 2013.
- [12] S. J. Jung, H. S. Shin, and W. Y. Chung, "Driver fatigue and drowsiness monitoring system with embedded electrocardiogram sensor on steering wheel," *IEEE Trans. Intell. Transp. Syst.*, vol. 8, no. 1, pp. 43-50, Feb. 2014.
- [13] F. -C. Lin, Ko L. -W. Ko, Chuang C. -H. Chuang, T. -P. Su, and C. -T. Lin, "Generalized EEG-Based Drowsiness Prediction System by Using a Self-Organizing Neural Fuzzy System," *IEEE Trans. Circuits Syst. I, Reg. Papers*, vol. 59, no. 9, pp. 2044-2055, Sep. 2012.
- [14] S. Hu, G. Zheng, and B. Peters, "Driver fatigue detection from electroencephalogram spectrum after electrooculography artefact removal," *IET Intell. Transp. Syst.*, vol. 7, no. 1, pp. 105-113, Mar. 2013.
- [15] X. Zhu, W. -L. Zheng, B. -L. Lu, X. Chen, S. Chen, and C. Wang, "EOG-based drowsiness detection using convolutional neural networks," *2014 International Joint Conference on Neural Networks (IJCNN)*, Beijing, China, 2014, pp. 128-134.
- [16] Y. Sun, and X. B. Yu, "An Innovative Nonintrusive Driver Assistance System for Vital Signal Monitoring," *IEEE Journal of Biomedical and Health Informatics*, vol. 18, no. 6, pp. 1932-1939, Nov. 2014.
- [17] M. Miyaji, H. Kawanaka, and K. Oguri, "Effect of pattern recognition features on detection for driver's cognitive distraction," *2010 13th International IEEE Annual Conference on Intelligent Transportation Systems*, Madeira Island, Portugal, 2010, pp. 605-610.
- [18] R. N. Khushaba, S. Kodagoda, S. Lal, and G. Dissanayake, "Intelligent Driver Drowsiness Detection System using uncorrelated fuzzy locality preserving analysis," *2011 IEEE/RSJ International Conference on Intelligent Robots and Systems*, San Francisco, USA, 2011, pp. 4608-4614.
- [19] G. Li, and W. -Y. Chung, "Detection of driver drowsiness using wavelet analysis of heart rate variability and a support vector machine classifier," *Sensors*, vol. 13, no. 12, pp. 16494-16511, Dec. 2013.
- [20] B. P. Nayak, and A. Routray, "A biomedical approach to retrieve information on driver's fatigue by integrating EEG, ECG and blood biomarkers during simulated driving session," *IEEE Proceedings of 4th International Conference on Intelligent Human Computer Interaction*, Kharagpur, India, 2012.
- [21] S. Heuer, B. Chamadiya, A. Gharbi, C. Kunze, and M. Wagner, "Unobtrusive in-vehicle biosignal instrumentation for advanced driver assistance and active safety," *2010 IEEE EMBS Conference on Biomedical Engineering & Sciences*, Kuala Lumpur, Malaysia, pp. 252-256, 2010.
- [22] K. T. Chui, K. F. Tsang, H. R. Chi, B. W. -K. Ling, and C. K. Wu, "Electrocardiogram based classifier for driver drowsiness detection," *13th IEEE International Conference on Industrial Informatics (INDIN2015)*, Cambridge, UK, 2015, pp. 600-603.
- [23] *Your Guide To Healthy Sleep*, National Institutes of Healthy, National Heart, Lung and Blood Institute, U.S., 2011.
- [24] N. Shrivastava, A. Khosravi, and B. Panigrahi, "Prediction interval estimation of electricity prices using PSO tuned Support Vector Machines," *IEEE Trans. on Ind. Informat.*, vol. 11, no. 2, pp. 322-331, Apr. 2015.
- [25] C. Lin, C. Mailhes, and J. -Y. Tournet, "P- and T-wave delineation in ECG signals using a Bayesian approach and a partially collapsed gibbs sampler," *IEEE Trans. Biomed. Eng.*, vol. 57, no. 12, pp. 2840-2849, Dec. 2010.
- [26] A. L. Goldberger, L. A. N. Amaral, L. Glass, J. M. Hausdorff, P. C. H. Ivanov, R. G. Mark, J. E. Mietus, G. B. Moody, C.-K. Peng, and H. E. Stanley, "PhysioBank, PhysioToolkit, and PhysioNet: Components of a new research for complex physiologic signals," *Circulation*, vol. 101, no. 23, pp. e215-e220, Jun. 2000.
- [27] V. N. Vapnik, *The nature of statistical learning*. Berlin: Springer, 1995.
- [28] B. -U. Kohler, C. Hennig, and R. Orglmeister, "The principles of software QRS detection," *IEEE - Engineering in Medicine and Biology Magazine*, vol.21, no.1, pp. 42-57, Jan.-Feb. 2002.
- [29] W. J. Tompkins, *Biomedical Digital Signal Processing C-Language Examples and Laboratory Experiments for the IBM®PC. ECG QRS Detection* (pp. 236-264), New Jersey: Prentice Hall, 2000.
- [30] C. M. Bishop, *Pattern recognition and machine learning*, New York: Springer, 2006.

- [31] K. T. Chui, K. F. Tsang, C. K. Wu, F. H. Hung, H. R. Chi, H. S. -H. Chung, K. F. Man, and K. T. Ko, "Cardiovascular diseases identification using electrocardiogram health identifier based on multiple criteria decision making," *Expert Systems with Applications*, vol. 42, no. 13, pp. 5684-5695, Aug. 2015.
- [32] R. Herbrich, *Learning kernel classifiers Theory and Algorithms*, London: The MIT Press, 2002.
- [33] V. A. Shim, K. C. Tan, and H. Tang, "Adaptive Memetic Computing for Evolutionary Multiobjective Optimization," *IEEE Trans. Cybern.*, vol. 45, no. 4, pp. 610-621, Apr. 2015.
- [34] Y. Wang, and Z. Cai, "Combining Multiobjective Optimization With Differential Evolution to Solve Constrained Optimization Problems", *IEEE Trans. Evol. Comput.*, vol. 16, No.1, pp. 117-134, Jan. 2012.
- [35] C. W. Hsu, and C. J. Lin, "A comparison of methods for multiclass support vector machine," *IEEE Trans. Neural Netw.*, vol. 13, no. 2, pp. 415-425, Mar. 2002.



Kwok Tai Chui (S'14) received the B.Eng. degree in electronic and communication engineering – Business Intelligence Minor, with first-class honor, from City University of Hong Kong in 2013, where he is currently working toward the Ph.D. degree. He was the recipient of 2nd Prize Award (Postgraduate Category) of 2014 IEEE Region 10 Student Paper Contest. Also, he received Best Paper Award in IEEE The International Conference on Consumer

Electronics-China, in both 2014 and 2015. His research interests include wireless communication, pattern recognition, healthcare, machine learning algorithms and optimization.



Kim Fung Tsang (M'95-SM'14) obtained his PhD degree from the Cardiff University of Wales, Cardiff, United Kingdom. He has close ties with industry, and is working actively on RFID (ZigBee) for numerous applications, including energy management system for utilities, metering infrastructure, security, and office/home automation. Dr Tsang has published more than 150 technical papers. He was the recipient of CityU's Applied Research Excellence Award, the first Hong

Kong Science & Product Innovation Competition and the World Chinese Invention Exposition. The other accolades won by Dr Tsang include the EDN Asia Innovator Award, Ericsson's Super-Wireless Application Award, the Best Award from Freescale Semiconductor, the Innovation China Outstanding Entrepreneur Award and the Excellent Product Award from the China Hi-Tech Fair.

Dr. Tsang is a Fellow of HKIE, Senior Member of IEEE and is now an Associate Professor as well as the Director of Wireless Sustainability Center in the Department of Electronic Engineering, City University of Hong Kong.



Hao Ran Chi (S'14) obtained the Bachelor of Engineering in Electronic and Communication Engineering with First Class Honor from City University of Hong Kong, in 2013. Currently, he is now studying for the Doctor of Philosophy at City University of Hong Kong. His research interests on artificial intelligence, optimization and wireless network.



Bingo Wing Kuen Ling (M'08–SM'08) received the B.Eng. (Hons) and M.Phil. degrees from the department of Electronic and Computer Engineering, the Hong Kong University of Science and Technology, in 1997 and 2000, respectively, and the Ph.D. degree in the department of Electronic and Information Engineering from the Hong Kong Polytechnic University in 2003. In 2004, he joined the King's College London as a Lecturer. In 2010, he joined the University of Lincoln as a Principal Lecturer and promoted to a Reader in 2011. In 2012, he joined the Guangdong University of Technology as a Full Professor.

His research interests include time frequency analysis and applications, optimization for life science, symbolic dynamics, fractal and chaos and control theories.



Chung Kit Wu received the B.Eng. degree in electronic and communication engineering, with first class honor, from City University of Hong Kong in 2014, where he is currently working toward the Ph.D. degree.

His research interests are beamforming, digital signal processing and network analysis.